Journal of Volcanology and Geothermal Research 431 (2022) 107639

Contents lists available at ScienceDirect

Journal of Volcanology and Geothermal Research

journal homepage: www.journals.elsevier.com/journal-of-volcanology-and-geothermal-research

New insights into carbon isotope systematics at Poás volcano, Costa Rica

Fiona D'Arcy [a,*], J. Maarten de Moor [b,c], John Stix [a], Alfredo Alan [d], Robert Bogue [a], Ernesto Corrales [d], Jorge Andres Diaz [d,e], Emily Mick [a], Jéssica Salas-Navarro [a], Romain Lauzeral [a]

[a] McGill University, Montreal, Canada
[b] OVSICORI, Universidad Nacional, Heredia, Costa Rica
[c] University of New Mexico, Albuquerque, NM, USA
[d] GasLAB, CICANUM, Universidad de Costa Rica, San José, Costa Rica
[e] INFICON Inc., Syracuse, NY, USA

ARTICLE INFO

Keywords:
Carbon isotopes
Volcanic gases
UAS gas sampling
Poás volcano
Geochemistry
Drones

ABSTRACT

In April 2017, an intense phreatomagmatic eruptive phase took place at Poás volcano in Costa Rica. This was the most significant eruptive activity at the volcano since the 1950's. Unlike previous eruptions, gas ratios were closely monitored during this event with the use of both ground-based MultiGAS and uncrewed aerial system (UAS) real-time monitoring, providing valuable insight into the nature of the eruption. This well-studied eruption presents a unique opportunity to examine hydrothermal and magmatic processes occurring at Poás during periods of unrest versus quiescent periods. Here, we present stable carbon isotopic results of volcanic CO_2 at Poás spanning the pre-eruptive as well as eruptive and post-eruptive phases in 2017 through 2019. Samples were collected by a combination of direct sampling (analyzed by Isotope Ratio Mass Spectrometry [IRMS] or Cavity Ring Down Spectroscopy [CRDS]), as well as UAS and ground-based plume sampling (analyzed by CRDS). Direct samples range from −6.17 to −3.73 ‰ during 2017 to 2019. Using the Keeling approach, we calculate $\delta^{13}C$ magmatic source values of −3.97 ± 1.94 ‰ and − 3.64 ± 0.48 ‰ using UAS sampling and ground-based sampling, respectively, for April 2019. We propose that these values for $\delta^{13}C$ are being governed by a combination of magmatic and hydrothermal fluctuations related to sealing and unsealing of the upper magma carapace. This process results in comparatively heavy values when the system is being buffered by fluid-gas interaction as the hydrothermal system seals and expands, while lightest values are predominant during unsealed phases where degassed magma supplies the volatiles along with phreatic or phreatomagmatic activity. The significance of this work is two-fold: it demonstrates the use of a rapid volcanic gas sampling strategy applicable for monitoring at other volcanoes prone to phreatomagmatic and/or phreatic eruptions, and it provides a new conceptual model to interpret the phreatic/phreatomagmatic eruptive activity at Poás over the last 20 years.

1. Introduction

Carbon isotopes are becoming a standard tool for assessing hydrothermal and magmatic processes through analysis of thermal waters (e.g. Venturi et al., 2017), calcite precipitates (e.g. Chiodini et al., 2015), soil gas (e.g. Hanson et al., 2018), fumaroles (e.g. Troll et al., 2012), fluid inclusions (e.g. Boudoire et al., 2018), and mantle minerals (e.g. Sandoval-Velasquez et al., 2021; Rizzo et al., 2018). Volcanic plumes are a valuable means of volcanic carbon isotopic monitoring at active volcanoes. Plumes represent a mixture of gases from a source or multiple sources along with background air at some distance from the vent, which means that with the right equipment, they can be safely and rapidly accessed during times of unrest. While dilute volcanic plumes have been sampled for subsequent isotopic analysis of carbon dioxide by helicopter (Fischer and Lopez, 2016) and from the ground (Schipper et al., 2017; Malowany et al., 2017; Chiodini et al., 2011; Rizzo et al., 2014, 2015), attempts to apply UASs (Uncrewed Aerial Systems) to this end are limited (Liu et al., 2020; Shingubara et al., 2021; Tsunogai et al., 2022). Nevertheless, UAS have proven to be vital to volcanological monitoring for topographic surveys, hazard mapping, instrument deployment, and gas measurements (James et al., 2020). In this work, we combine direct sampling of fumaroles with indirect volcanic plume

* Corresponding author at: McGill University, Montreal, Canada.
E-mail address: fiona.darcy@mail.mcgill.ca (F. D'Arcy).

https://doi.org/10.1016/j.jvolgeores.2022.107639
Received 5 November 2021; Received in revised form 1 July 2022; Accepted 31 July 2022
Available online 3 August 2022

sampling both from the ground and by UAS at Poás volcano, Costa Rica, to characterize the stable carbon isotopic variations in the volcanic CO_2. We draw comparisons between the two methods and use our extensive suite of samples to provide new insight into the processes governing the magmatic-hydrothermal interactions at Poás.

Poás volcano is one of Central America's most dynamic volcanoes. It is characterized by cycles of phreatic and phreatomagmatic activity centered around a dome and crater which has hosted an intermittent crater lake (Laguna Caliente) closely monitored since 1980 (e.g. Martínez et al., 2000; Rowe et al., 1992; Rouwet et al., 2017). Changes in crater lake level have been associated with shallow intrusions in 1981 beneath the dome, and in both 1985–1990 and 1998–2004 beneath the lake-filled pit crater (Rymer et al., 2005; Rymer et al., 1998). Currently, CO_2, SO_2, and H_2S are the main gases used to monitor the activity of Poás by MultiGAS and other methods (e.g. Fischer et al., 2015; de Moor et al., 2016; de Moor et al., 2019; Vaselli et al., 2019). Large changes in SO_2/CO_2 are interpreted to be driven by variations in SO_2 flux due to interactions between S-rich magmatic gas and acid hydrothermal fluids (de Moor et al., 2019). This process is common in other volcanic systems which host crater lakes, such as Ruapehu (Christenson et al., 2010) and Rincón de la Vieja (Battaglia et al., 2019). In these sulfur-rich environments, small variations in CO_2 flux are less useful as a monitoring tool because they are eclipsed by larger variations in sulfur and have large associated errors. On the other hand, carbon isotopic compositions of gas emissions are unaffected by fluctuations in sulfur, so they are sensitive to small changes in CO_2 sources or fractionation processes, making them a useful monitoring tool in these systems.

The April 2017 phreatic and phreatomagmatic activity at Poás resulted in the drying out and disappearance of the Laguna Caliente and destruction of most of the adjacent pyroclastic dome structure (Vaselli et al., 2019). This was the most significant eruptive activity since the 1950's, and juvenile magmatic material of andesitic composition (~57.4 wt% SiO_2; de Moor et al., 2019) was expelled during these eruptions. During the present study, Poás crater contained a large vent ("Boca A" produced by the 2017 eruption and destruction of the dome) emitting a near constant, highly convective gas plume. Hosted within the bed of the previous crater lake were two smaller flooded vents occupied by vigorously bubbling S-rich pools (Boca C) and an adjacent fumarole field (Boca B; Fig. 1). The dynamic environment of the crater of Poás poses a challenge to long-term monitoring of gases, as different sites have appeared and disappeared over the years, preventing robust comparison among different studies (Vaselli et al., 2019). In order to compare spatial variations, we collected $\delta^{13}C$ results from samples taken across five sites in the active crater area within a 5-day time period in 2019, ranging from the ambient plume to diffuse degassing from the bed of the previous crater lake. Measurements of $\delta^{13}C$ from fumaroles at Poás were reported from 2000 to 2004 (Vaselli et al., 2019) and from 2001 to 2008 (Hilton et al., 2010); here we report a new time series of measurements spanning January 2017 to April 2019. We use the isotopic data reported here for 2017 to 2019, in conjunction with gas ratios reported elsewhere, to build a new conceptual model involving hydrothermal buffering and degassed shallow magma which we apply to activity at Poás spanning the last 20 years.

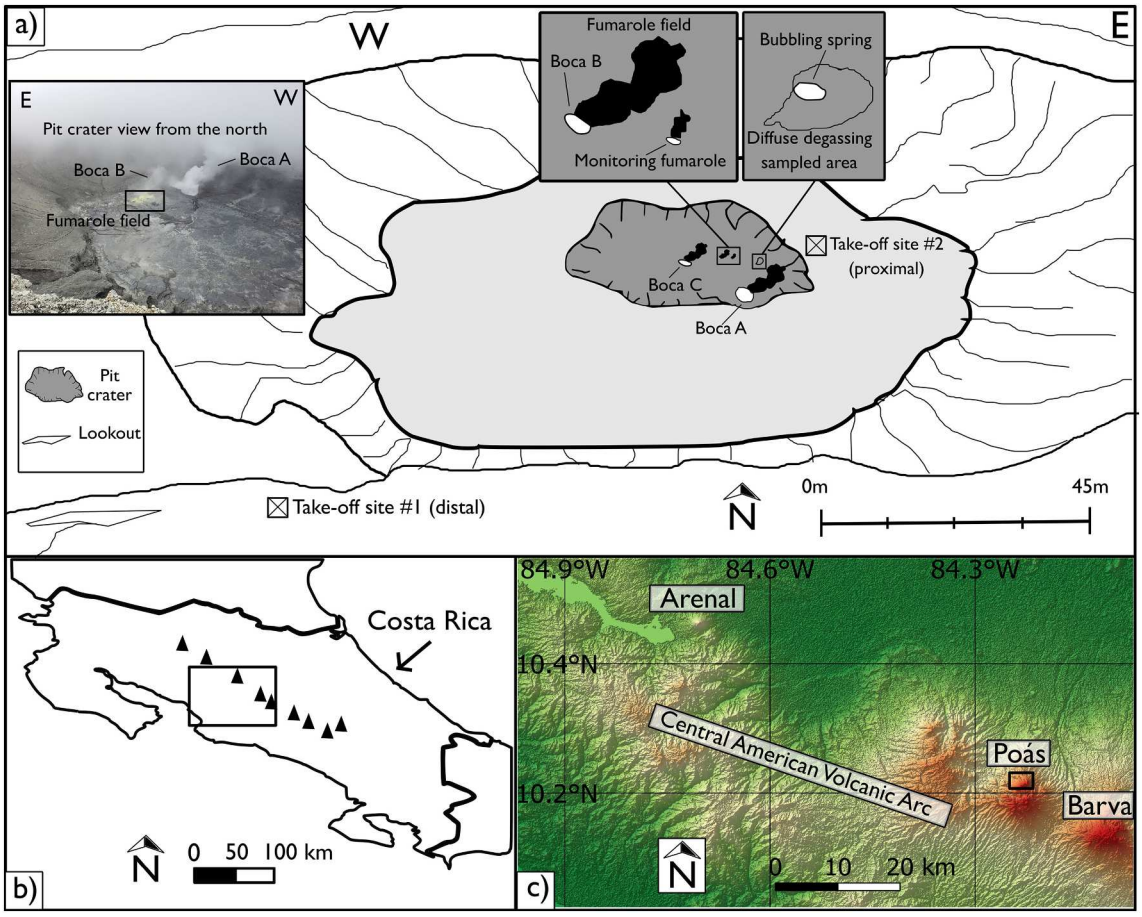

Fig. 1. (a) Map showing the location of takeoff site #1 and #2, Boca A, Boca B, Boca C, the monitoring fumarole, bubbling spring, and diffuse degassing area. (b) General location of Poás volcano in Costa Rica. (c) Location of Poás volcano with respect to the Central American Volcanic Arc (CAVA) as an inset of the box outlined in (b). DEM data for (c) was generated using Advanced Spaceborne Thermal Emission and Reflection Radiometer (ASTER) Global 341 Digital Elevation Model (GDEM) data, a product of METI and NASA.

2. Material and methods

Direct samples were obtained from February 2017 through February 2019 with Giggenbach bottles (Giggenbach, 1975). Fumaroles were sampled with a titanium tube, and bubbles emanating from the crater lake and subsequent isolated pools were collected using an inverted funnel. Gases were bubbled through a 4 N NaOH solution in a glass Giggenbach bottle and returned to the lab at OVSICORI, where this solution was extracted and oxidized. Aliquots of 0.5 ml of the oxidized solution were then introduced into 12 ml exetainer vials. These samples were then acidified using 30% orthophosphoric acid by an automated autosampler and resulting CO_2 gas was analyzed by Cavity Ring-Down Spectrometry. All other samples were collected in 2019 from 25 to 30 April using UAS plume sampling, ground-based plume sampling, and direct sampling and subsequently analyzed by Cavity Ring-Down Spectrometry.

2.1. UAS plume sampling

We collected UAS samples on two days, a distal sampling campaign on 25 April 2019 and a proximal campaign on 30 April. The distal UAS sampling assembly (Fig. 2A) was used on 25 April during five sampling flights of the plume taken 20 to 100 m above the pit crater. Take-off and landing took place from take-off site #1 at the lookout or "Mirador" where tourists gather (Fig. 1). The assembly consisted of a quadcopter (TurboAce Matrix-i) and flight time of ~10 min with payload comprising the gas sampling configuration attached on top of the UAS body and secured with bungee cords, while gas sample bags were attached directly below the drone. The payload (700 g) consisted of a pump (micropump®, model d3k, 2.5 L/min) connected to an electronic switch (Turnigy 10A/30 V) which utilized an empty standard port on the UAS receiver. An SO_2 sensor (Citicell 0–200 ppm range) was included with a voltage sensor (Futaba SBS-01 V) connected to the SBUS2 port of the receiver and one of the inlet tubes of the pump. A portable USB-powered charger supplied power to the pump while a 9 V battery powered the SO_2 sensor. The four sampling bags (Altef, 800 ml) were connected in series via the outlet tube of the pump and contained in a mesh bag connected by a carabiner and 0.1 m rope under the drone. The pump switch and SO_2 sensor were mapped to channels on the remote controller for the drone, allowing the pilot to use two-way telemetry to read the voltage of the SO_2 sensor and turn the pump on and off for sampling.

The proximal UAS sampling assembly (Fig. 2B) was used on 30 April during three sampling flights of the plume 10–20 m above the fumarole field. Take-off and landing occurred from take-off site #2 located within the crater, adjacent to the previous site of the crater lake (Fig. 1). The assembly consisted of a quadcopter (DJI Inspire 1, flight time of ~6 min with payload) with the gas sampling configuration as a separate unit suspended 1.5 m below the UAV. The payload (360 g) consisted of a pump (1.2 L/min) connected to an electronic switch (Turnigy 10A/30 V) and a stand-alone receiver (Futaba R70087B) along with a battery pack. The four sampling gas bags (Altef, 800 ml) were connected in series from the outlet tube of the pump and contained in a mesh bag along with the gas sampling unit. The UAS was maneuvered with one remote controller by the pilot, while the gas sampling unit was controlled by a second person using a secondary remote controller to switch the pump on and off. The convective nature of Boca A and Boca B prevented UAS sampling from those plumes at this proximal location.

2.2. Ground-based plume sampling

On 26 and 30 April, near-source ambient plume samples were taken in the fumarole field by placing the inlet tube on top of boulders in the fumarolic plume and using a pump to purge 5 m of tubing before filling sample bags (Fig. 1). The plumes of Boca A and Boca B were sampled at ground level by extending the inlet tube horizontally and using the

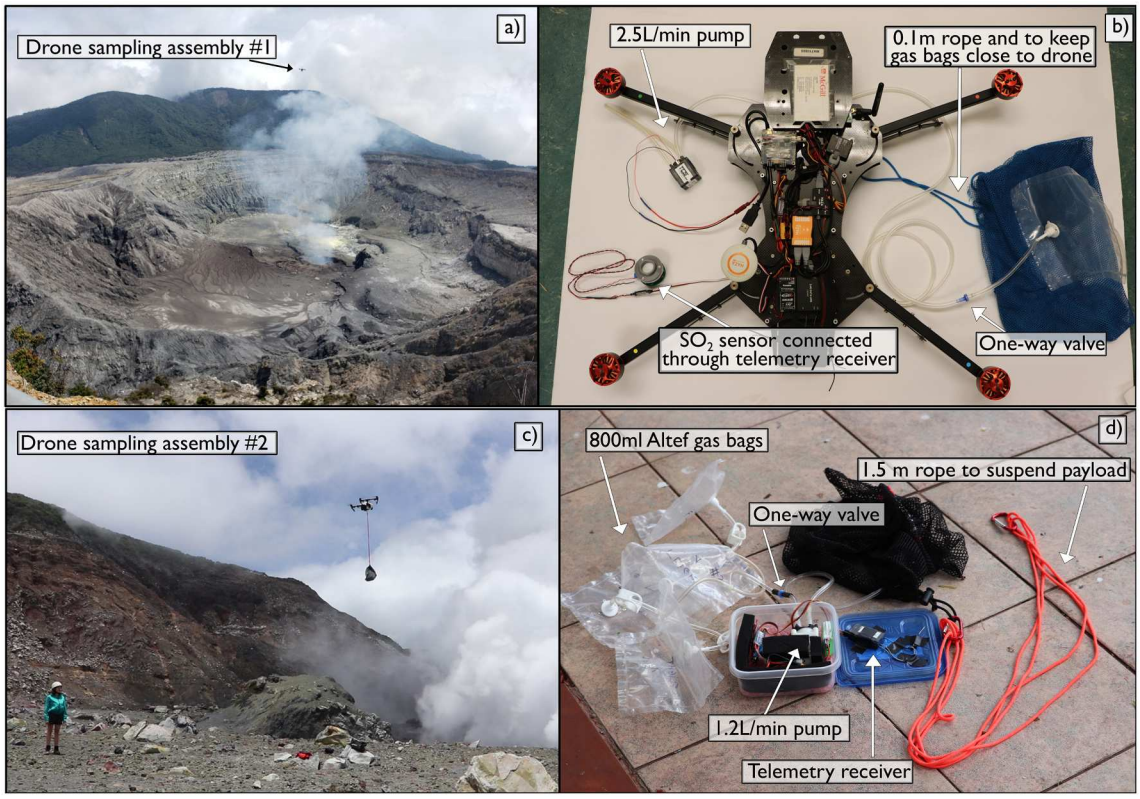

Fig. 2. Sampling assembly by UAS used at Poás in April 2019. a) Distal assembly used for sampling the volcanic plume on 25 April b) Distal assembly components and specifications. c) Proximal assembly used for sampling at Poás crater on 30 April 2019. d) Proximal assembly components and specifications.

pump to purge the line before filling sample bags.

2.3. Direct sampling

On 30 April, direct samples were collected in replicates of five within the floor of the pit crater from the monitoring fumarole, from a tube inserted into warm ground, and from a bubbling pool (Fig. 1). A titanium tube or funnel was connected to <1 m of silicon tubing, and a 1000 ml syringe and 3-way valve were used to flush the line of ambient air prior to collecting the sample. Each 12 ml vial was then flushed three times and filled to overpressure.

2.4. Isotopic analysis

All samples from 25 to 30 April were analyzed within 24 h on a Picarro G2201-i CRDS at the geochemistry lab of the Observatorio Vulcanológico y Sismológico de Costa Rica (OVSICORI) in Heredia, Costa Rica, following the methods of Malowany et al. (2017). A copper tube filled with fine copper wire cuttings was used to remove any interference from H_2S, and three in-house standards (−43.15‰, −15.6‰, and − 11.4‰) were used to define a calibration curve (Fig. S1). Any samples above 5000 ppm CO_2 were diluted with zero air administered from a tank using a gas-tight syringe. A standard was run every 5 to 12 samples at concentrations ranging from 450 to 1050 ppm CO_2 to monitor instrument drift (Table S1). Carbon isotopic results are reported using the per mil notation which provides values relative to the Vienna Pee Dee Belmenite (VPDB) reference standard. Repeat analysis of standards shows that uncertainties are ~0.3 ‰.

3. Results

3.1. UAS and ground-based $\delta^{13}C$ results of April 2019

Results of all carbon isotopic measurements collected at Poás during 25–30 April 2019 are reported in Table S1 and direct samples from 2017 to 2019 are reported in Table S2. A background flight and unaffected ground samples ranged from 406 to 411 ppm and $\delta^{13}C$ of −9.5 to −10.4 ‰. Therefore, average background in this location during the time of sampling was 408 pm and − 9.8 ‰. This is within an acceptable range for the tropospheric region, whose atmospheric signature varies, even at remote summits, due to diurnal fluctuations from biogenic respiration and altitude (Takahashi et al., 2002; Araujo et al., 2008). On 25 April, 16 dilute plume samples were collected by distal UAS sampling, with CO_2 concentrations ranging from 408 ppm to 491 ppm, and $\delta^{13}C$ of −9.7 to

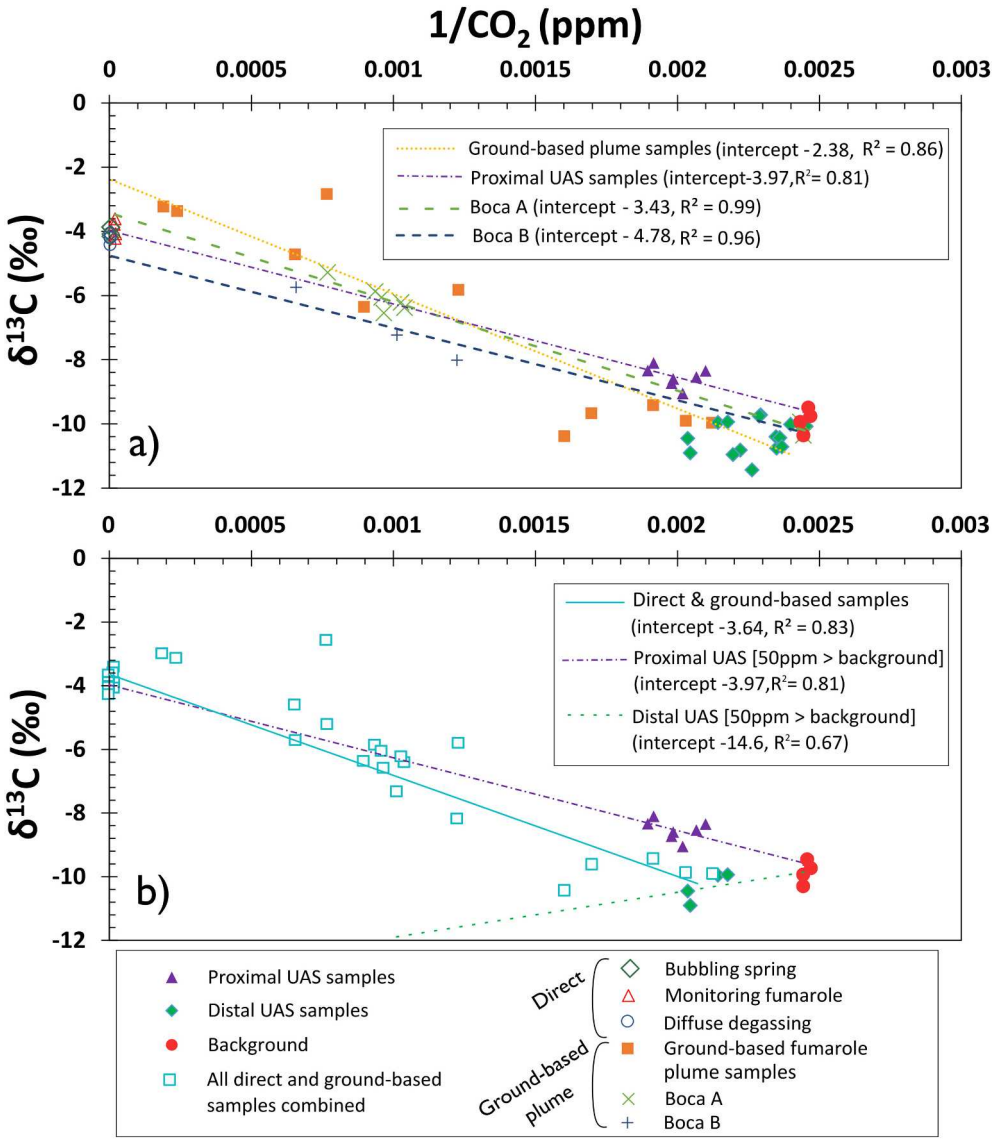

Fig. 3. Plots showing inverse CO_2 concentration versus $\delta^{13}C$ relative to Vienna Pee Dee Belemnite of gas samples collected at Poás volcano in April–May 2019. a) Proximal UAS sampling (solid triangles), Boca A (x's), Boca B (crosses), and fumarole field plume samples (solid squares) are shown along with their line of best fit. Also shown are samples from the distal UAS (solid diamonds), along with measurements of background air taken at the site (solid circles). Lastly, direct samples with very high concentrations are plotted as diffuse degassing (open circles), bubbling spring (open diamonds), and monitoring fumarole (open triangles). b) All ground-based sampling, including direct samples and samples of diffuse plumes taken from the ground, are plotted together (open squares) for comparison with proximal UAS sampling (triangles) and distal UAS samples (diamonds) >50 ppm above background along with their respective linear regression lines of best fit.

−11.4 ‰. On 30 April, 8 dilute plume samples were collected by proximal UAS sampling, with CO_2 concentrations ranging from 477 ppm to 528 ppm, and $\delta^{13}C$ of −8.2 to −9.1 ‰. On 26 and 30 April, we collected a total of 37 ground-based samples from the ambient plumes of Boca A, Boca B, and the fumarole field, with CO_2 concentrations ranging from 570 ppm to 5280 ppm and $\delta^{13}C$ of −3.2 to −10.4 ‰. Direct samples from 30 April taken from the monitoring fumarole, bubbling spring, and diffusely degassing soil range from −3.9 to −4.7 ‰. Concentrations exceed 40,000 ppm CO_2 for all direct samples.

The results of both the UAS proximal sampling and ground-based sampling are compared in Fig. 3A and B. We used a Keeling approach (Keeling, 1958) to model a binary mixing line between background air and the volcanic source in order to estimate the volcanic source $\delta^{13}C$. Using this method, we performed regression analysis for proximal UAS samples ($n = 10$, −3.97 ± 1.94 ‰, R^2 of 0.81), Boca A samples ($n = 6$, intercept of −3.42 ± 0.49 ‰, $R^2 = 0.99$), Boca B samples ($n = 3$, intercept of −4.76 ± 1.5 ‰, $R^2 = 0.96$), and ground-based sampling of the plume above the fumarole field ($n = 11$, intercept of −2.38 ± 1.5 ‰, $R^2 = 0.86$). Errors on the intercepts are calculated at 95% confidence. In Fig. 3A, the intercept of the proximal UAS-based sampling falls within the range of source values estimated for Boca A, Boca B, and the fumarole field, indicating the UAS was sampling a mixed plume. The proximal UAS intercept (−3.97 ‰) is nearly identical to the direct sampling $\delta^{13}C$ (average − 4.01%). In Fig. 3B, all ground-based samples from April 2019 (Boca A, Boca B, ground-based samples above fumarole field, and direct samples) are grouped together as a mixed population to compare with the UAS results. The mean $\delta^{13}C$ estimated for all ground-based samples is −3.64 ± 0.48 ‰ ($n = 33$, R^2 of 0.83), a difference of 0.33 ‰ from the source value based on the proximal UAS samples. Also in Fig. 3B, we compare proximal UAS samples (all of which are >50 ppm above background) with distal UAS samples >50 ppm above background. We performed a linear regression on distal UAS samples of 25 April, to delineate a ternary source (−14.6 ± 4.4 ‰, $R^2 = 0.67$, $n = 4$). As the distal samples were collected in less dense volcanic plume up to 100 m above the vents, we postulate that these samples are a mixture of volcanic emissions (−4‰, this work), soil respiration from the crater floor (−17 to −27 ‰; Glamoclija et al., 2004), forest or pasture respiration from adjacent areas (−27 or − 21 ‰, respectively; (Powers, 2006), and stable atmosphere (−8.5 ‰; White et al., 2015). For this reason, these samples are plotted along with their own regression line, and are not included in the proximal regression.

In Fig. 4, ground-based sampling from the three direct sampling sites in 2019 are compared to Boca A and B plumes. There is no statistically significant variation of $\delta^{13}CO_2$ for sites at Poás volcano measured in our study within the same 5-day span. This is consistent with the lack of significant $\delta^{13}CO_2$ variation among three fumaroles sampled from 2001 to 2008 (Hilton et al., 2010) and lack of systematic differences in major gas geochemistry from the same three sites (Fischer et al., 2015). However, de Moor et al. (2016) showed that SO_2/CO_2 varies between sources within the crater mostly due to variations in SO_2 flux. While we cannot rule out the possibility that the sites sampled in our study are isotopically distinct, we use the average $\delta^{13}C$ (−4.1 ± 0.5 ‰) collected in our study to represent the carbon isotopic signature of Poás volcano in April 2019 for temporal comparison with results from previous sample periods.

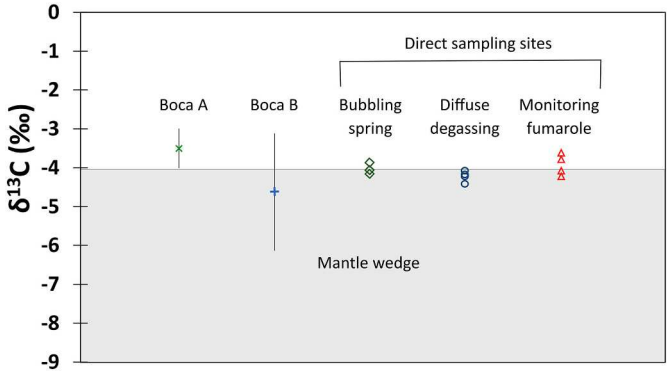

Fig. 4. Spatial comparison of $\delta^{13}C$ in gas samples among sampling sites within the pit crater at Poás. Individual samples are shown for the monitoring fumarole (open triangles), bubbling spring (open diamonds) and diffuse degassing (open circles). Due to the comparatively dilute samples, the intercept of a linear regression of samples are shown for Boca A (green x's) and Boca B (blue crosses) along with the associated 95% confidence interval for each intercept (vertical lines). Mantle value shown is world-wide MORB (Sano and Marty, 1995). (For interpretation of the references to colour in this figure legend, the reader is referred to the web version of this article.)

3.2. Direct sampling results of January 2017 to April 2019

Direct samples range from −3.7 to −6.2 ‰ during 2017 to 2019, with the lightest value of −6.2 ‰ observed one week before the initiation of the April 2017 phreatic to phreatomagmatic activity (Fig. 5) during a ramping up phase of unrest associated with increasing SO_2 flux, increasing SO_2/CO_2 ratio, elevated seismicity, and inflation (Salvage et al., 2018; de Moor et al., 2019). These values lie within the range obtained for 2001 to 2008 samples (−1.3 to −6.8 ‰) from Hilton et al. (2010) and within the range of those obtained for 2000 to 2004 samples (−2.6 to −6.2 ‰) from Vaselli et al. (2019). With the exception of the April 2017 value of −6.2 ‰, a baseline during 2017 to 2019 appears to range between −3.4 and − 5.1 ‰ for our dataset. The notably low value in April 2017 falls within the range of $\delta^{13}C$ recorded by Hilton et al. (2010) in January to July 2001 (−5.6 to −6.8 ‰). Fischer et al. (2015) interpreted unstable fluctuations in gas ratios during 1998 to 2001 as the result of an influx of magmatic volatiles that occurred prior to 2001 along with increased infiltration of surface waters due to hydrofracturing events.

4. Discussion

Certain phreatic and phreatomagmatic eruptions are inherently linked to failure of a semi-permeable mineralized cap known as a hydrothermal seal (Mick et al., 2021; Stix and de Moor, 2018). This porosity-reducing mineralization has been considered by Rowe et al. (1992), notably for native sulfur deposits, in their model of a fractured magma carapace at Poás volcano. One caveat to consider when monitoring for magmatic changes at volcanoes with hydrothermal systems is the possibility of gases and their isotopic ratios being buffered by the hydrothermal system (Tassi et al., 2016). This further highlights the need to recognize which results indicate magmatic unrest and which are indicative of hydrothermal buffering. Our work attempts to unravel this issue, laying the foundation for future studies exploring this interaction at Poás and elsewhere. Given the explosive nature of these eruptions, we first discuss how the use of UAS can improve monitoring at volcanoes with dynamic magmatic-hydrothermal systems. Next, we discuss the possible controls on carbon which could be related to magmatic fluids and sources, degassing, or hydrothermal sealing and unsealing at Poás. Finally, we integrate each of these controls into a new model incorporating the carbon isotope and gas ratio data from the 2005–2006 and 2017–2019 activity.

4.1. Drone-based and direct CO_2 sampling for same-day stable carbon isotopic analysis

An inherent challenge to airborne $\delta^{13}CO_2$ sampling of plumes is dictated by the need to sample a relatively high concentration plume, which is usually turbulent and risky to sample by UAS. Our work demonstrates that sampling dilute volcanic plumes by UAS can be a feasible volcano monitoring tool, which could supplement time-intensive ground sampling from crater floors. While the low CO_2 flux

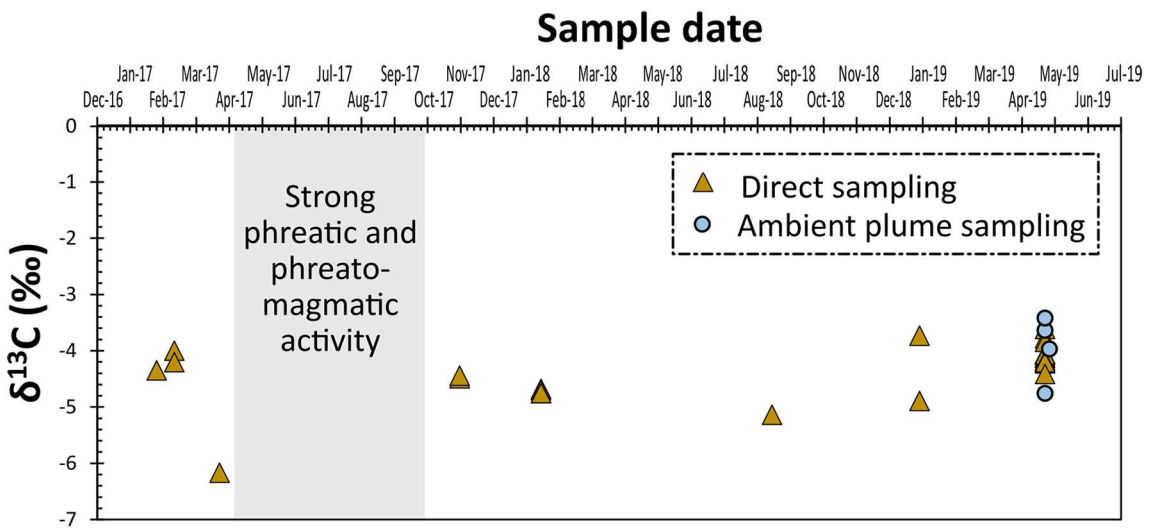

Fig. 5. Carbon isotopic ratios relative to Vienna Pee Dee Belemnite from 2017 to 2019 at Poás volcano. Triangles represent direct sampling points collected from fumaroles, bubbling point source, or diffuse degassing through crater soil and measured by CRDS or IRMS. Circles represent estimates of source $\delta^{13}C$ for various plumes sampled by ground-based or UAS methods and extrapolated using the Keeling method (1958).

at Poás limited the concentration of dilute plume samples we collected in April 2019 (406 ppm to 528 ppm CO_2), we sampled higher concentrations and mole fractions of volcanic CO_2 (120 ppm above background, 23%, this work) as compared to other UAS carbon isotopic sampling campaigns at Manam volcano, Papua New Guinea (85 ppm above background, 21%; Liu et al., 2020) and at Aso volcano, Japan (98 ppm above background, 19%; Tsunogai et al., 2022). Using linear regression, we found remarkably similar $\delta^{13}C$ volcanic source values with the drone gas sampling assembly as compared to high concentration direct sampling. To further cross-validate our source estimate, we compared the linear regression using all proximal UAS samples (-3.97 ± 1.95 ‰, $R^2 = 0.81$) to that of only proximal samples with CO_2 concentrations >500 ppm (-3.88 ± 1.55 ‰, $R^2 = 0.93$,) which are in agreement to within 0.09 ‰. Finally, we use a weighted mean of individual estimates based on proximal samples with CO_2 concentrations >500 ppm (Schipper et al., 2017), which estimates the volcanic signature to be -3.22 ± 0.86 ‰, thus within the acceptable error range produced by either regression calculation (Table S3). With caution and good sampling conditions, UAS plume sampling for isotopic analysis of carbon can be a reliable means by which to estimate the carbon signature at the source of a volcanic vent.

4.2. Controls on carbon isotopic systematics

Our data from 2017 to 2019 shows a marked change in baseline CO_2 in the lead-up to the April 2017 eruptive period. We propose that a steady-state convecting magma chamber replenished by deep injections governs the observed range in $\delta^{13}C$ baseline values (3.4 to −5.1 ‰). Minor variations in supply and increased magmatic fluids could potentially account for the slight rise in the baseline $\delta^{13}C$ leading up to the 2017 activity. However, this model alone cannot explain the major drop in $\delta^{13}C$ (from baseline to −6.2‰) observed at Poás in the immediate weeks leading up to the April 2017 opening eruptive phase. There are three main types of controls on carbon which we consider to interpret this drop in $\delta^{13}C$: deep sources of carbon, fractionation during magmatic degassing, and fractionation during shallow hydrothermal processes.

The simplest mechanism to begin with is based purely on fingerprinting the sources of carbon that supply the magmatic system from which the CO_2 is derived. The relative abundances of mantle wedge, sediment, and limestone accrued during subduction can be estimated based upon $\delta^{13}CO_2$ and CO_2 /^{3}He (Sano and Marty, 1995). Based upon further $^3He/^4He$ records, Hilton et al. (2010) postulated that beyond these three endmembers, crustal-derived CO_2 from the Caribbean plate could have caused the observed increase in $\delta^{13}CO_2$ in fumaroles at Poás from 2001 to 2005. Isotopically light compositions were attributed to relatively higher mantle contribution to the magmatic system. However, this model does not apply to our 2017 to 2019 data given the evidence for a lack of deep magma involved in the eruption. The evolved composition of the juvenile magma erupted in the 2017 eruption (de Moor et al., 2019) and high SO_2/CO_2 concurrent with phreatic-phreatomagmatic eruptions reported during 2014 to 2017 at Poás (de Moor et al., 2016; de Moor et al., 2019) together provide evidence for remobilization of pre-emplaced magma rather than injection of a fresh CO_2-rich intrusion spawning the 2017 activity. Finally, deep supply of CO_2 from increased magmatic fluids in 2017 would be expected to supply a more positive $\delta^{13}C$, so we instead seek other processes to explain the negative $\delta^{13}C$ excursion of April 2017.

The second mechanism we expore is fractionation during magma degassing. Experimental studies have shown that $\delta^{13}CO_2$ decreases as a magma becomes progressively more degassed (Holloway and Blank, 1994), due to the preferential exsolution of heavier carbon into the vapor phase (Javoy et al., 1978). In Hawaii, Gerlach and Taylor (1990) demonstrated that closed-system equilibrium degassing can account for carbon isotope fractionation leading to the more negative $\delta^{13}CO_2$ of the Kilauea East Rift zone (−7.8‰) as compared to less fractionated summit crater gases (−3.4‰). At Etna, several authors have noted decadal or annual variations in $\delta^{13}CO_2$ which have been attributed to a combination of either deep and shallow magmatic endmembers of different stages of degassing being tapped, carbonate assimilation over time, or mantle metasomatism of carbon-rich fluids (Chiodini et al., 2011; Paonita et al., 2012; Martelli et al., 2008). Short-term variations in $\delta^{13}CO_2$ at Etna spanning 5 days were attributed solely to degassing-associated fractionation (Rizzo et al., 2015). A dual magmatic source has been extensively studied at Stromboli volcano (Aiuppa et al., 2010) whereby explosive periods are supplied by CO_2-rich gas bubbles from a deep source while degassing of a shallow magma contributes to quiescent degassing. Injection of deeply sourced CO_2 from undegassed basaltic magma would be expected to produce isotopically heavier CO_2 (more positive $\delta^{13}CO_2$ than baseline) (Javoy et al., 1978) rather than the observed negative $\delta^{13}CO_2$ of −6.2 ‰. Our sample from April 2017 shows an anomalously light $\delta^{13}C$ consistent with the idea that the CO_2 was released from a largely degassed magma (de Moor et al., 2019) which was emplaced at shallow levels in 2000–2005 (Rymer et al., 2009).

There is a third mechanism of potentially equal importance at Poás:

shallow buffering of carbon. In a hydrothermal setting, carbon can theoretically exist in gaseous, solid (bound in minerals), or aqueous (dissolved in solution) form. Preferential uptake of carbon during exchange from one form to another can result in fractionation corresponding to a fractionation factor, ε, which is dependent on temperature. In systems where pH is neutral or higher, calcite deposition in hydrothermal alteration areas is a mechanism by which CO_2 is removed from solution (Giggenbach, 1984). Assuming precipitation at temperatures <192 °C, hydrothermal calcite deposited in the hydrothermal system will be isotopically heavy with respect to the gas (Ray et al., 2009; Barry et al., 2019). If calcite were dissolved back into hydrothermal fluids and released as a gas phase, we would expect an increasingly heavy signature. However, Laguna Caliente at Poás is highly acidic (Martínez et al., 2000), and no calcite has been found in a recent study which surveyed the alteration minerals in the surficial area (Rodríguez and van Bergen, 2017). Carbon dioxide exsolved from a magma body can remain in gaseous form or become dissolved in hydrothermal fluids according to Henry's law of solubility (Vogel et al., 1970). In the low pH settings of active craters, the aqueous form will be almost exclusively dissolved carbon, as bicarbonate and carbonate speciation is negligible. The ^{13}C partitions preferentially into the vapor phase according to a fractionation factor, $\alpha^{13}CO_2^{\text{vapor-solution}}$ which is temperature-dependent. As the core acid part of the hydrothermal system expands and is heated, fluid-gas fractionation could contribute isotopically heavy C to the gas emissions. This has been postulated for hydrothermal areas exhibiting heavier $\delta^{13}CO_2$ as compared to higher-temperature crater areas at Turrialba volcano (Malowany et al., 2017). We propose that this hydrothermal process could potentially account for the slight rise in the baseline $\delta^{13}C$ leading up to the 2017 activity.

We now formulate our model of the activity at Poás in relation to the sealing and unsealing of the hydrothermal cap while drawing upon the fundamental mechanisms discussed above.

4.3. Spatio-temporal evolution of carbon isotopic variations at Poás from 2017 to 2019

We first discuss the implications of our results in terms of spatial variation at the study site, then discuss temporal evolution. While we cannot say for certain whether the different sources in the Poás crater are isotopically homogeneous due to the overlap in error among Boca A, Boca B, and the fumaroles (Fig. 4), we can see that these sites may be supplied with gases from a common source with $\delta^{13}CO_2$ of -4.1 ± 0.5 ‰. The limited spatial variation could indicate a common permeable conduit source which is comprised of a network of interconnected fractures, as has been proposed to explain intra-crater spatial variation elsewhere, e.g., Cerro Negro (Lucic et al., 2014). This aligns well with the proposed structure of the magmatic plumbing system at Poás proposed by Rymer et al. (2005), wherein gravimetric data point to a common magmatic carapace that is overlain by finger-like intrusions of shallower magma <100 m beneath the pit crater and dome. Keeping in mind the uncertainty of spatial variations, we now compare temporal results of carbon isotopes collected from various locations at Poás in this campaign (2017 to 2019) to previous campaigns (2001 to 2014).

The first stage of activity which our data cover is January to March 2017, when the gases were supplied by a convecting magma chamber overlain by a relatively well-sealed hydrothermal system. High H_2S/SO_2 and increasing C/S indicate hydrothermal sealing processes associated with sulfur deposition, while $\delta^{13}C$ remains within baseline values. Failure of the hydrothermal seal in April 2017 likely caused sudden depressurization of previously emplaced shallow magma and was associated with increased degassing (de Moor et al., 2019). The next stage of activity is the April 2017 phreatomagmatic episodes and subsequent eruptions through August 2017. The onset of the eruption caused the hydrothermal seal to break, allowing the shallow magmatic gas which had been accumulating in the volatile-rich zone of the magma carapace to escape. Since the magma carapace was emplaced pre-2006 (Rymer et al., 2009; Fischer et al., 2015), the magma had already been degassing for several years. These observations agree with our results, wherein the $\delta^{13}C$ dipped to a more negative value (−6.2 ‰) consistent with a greater influence from a degassed magma. By November 2017, the $\delta^{13}C$ had returned to within baseline values (−4.5 ‰), indicating a return to steady state conditions as the hydrothermal seal was steadily rebuilding.

Extending our model further into the past, we now provide a new interpretation of the 2001–2008 evolution of carbon isotope systematics at Poás. In Fig. 6 we compare data taken from gases at the Naranja/Norte fumarole, Official/Este fumarole, and Monitoring fumarole (Hilton et al., 2010; Fischer et al., 2015; Vaselli et al., 2003, 2019) with our data. Firstly, the lowest $\delta^{13}C$ of 2001 (−4.3 to −6.8 ‰) was collected from the Official/Este fumarole (Vaselli et al., 2019; Fischer et al., 2015) and is equivalent to the April 2017 isotopic signature (−6.2 ‰) of degassed magma with little or no hydrothermal influence. H_2S/SO_2 was low in 2001, consistent with a lesser influence of the hydrothermal system, though spatial heterogeneity is apparent. Scatter in the carbon isotopic values also reflects spatial heterogeneity in those fumaroles closer to the lake which likely underwent some buffering during gas-fluid exchange processes. The $\delta^{13}C$ then increased from January 2001 to June 2005, peaking at −1.3 ‰ in June 2005, 9 months before the first phreatic eruption in 2006. This was followed by a steady decrease in $\delta^{13}C$ during phreatic activity post-June 2005, reaching −4.0 ‰ by 2008. This could be explained by either the shallow (fluid-gas interaction) or deep (degassing fractionation) mechanisms considered in our model. The first scenario suggests that the peak in $\delta^{13}C$ of −1.3‰ in 2005 was a response to increased heat, expansion of the acidic hydrothermal system and an increasing fluid-gas fractionation prior to the current extended eruption period. The second scenario would suggest that the increasing $\delta^{13}C$ was caused by progressively greater influence from the deeper system as slab and mantle carbon has a $\delta^{13}C$ of −0.5‰ (Barry et al., 2019). As injections of undegassed magma enter into the deep convecting magma chamber with associated emplacement of shallow dikes, $\delta^{13}C$ would increase, while the subsequent decrease in $\delta^{13}C$ would be due to degassing fractionation as CO_2 is lost from those same dikes. Both these scenarios align well with the model suggested by Fischer et al. (2015) in which injection of magma or magmatic volatiles in 1998 to 2005 were marked by increased C/S (Fig. 6), which progressively formed a hydrothermal seal and subsequent pressure buildup under the seal. According to these authors, the post-2006 magma was continuously degassing and the hydrothermal seal became fractured as phreatic eruptions occurred in 2006 and 2008, with intermittent re-sealing. In late 2006, $\delta^{13}C$ values were − 4 to −5 ‰, indicating a transition between partly hydrothermal and partly magmatic influence. More recently, Vaselli et al. (2019) suggested overpressuring and rupture of the hydrothermal seal in 2005–2006 as the system switched from hydrothermal to more magmatic dominated. Our model strengthens previous models by incorporating a mechanism by which carbon isotope systematics can be accounted for during both magmatic-dominated eruptive phases and baseline hydrothermal activity. With this new insight, we can now better understand and recognize the cycles of hydrothermal seal formation and pressurization leading up to phreatomagmatic activity using carbon isotope monitoring.

5. Conclusions

Our new UAS approach to volcano monitoring could fill the gap left by current techniques, as rapid and repeated deployment of sampling drones, with same-day isotopic analysis, can be used prior to, during, and after eruptive phases to detect small isotopic changes occurring in the magmatic-hydrothermal plumbing system which would otherwise be overlooked. We have combined direct sampling of fumaroles with ground-based and UAS-based sampling of volcanic plumes at Poás volcano, Costa Rica, to characterize the stable carbon isotopic variations in

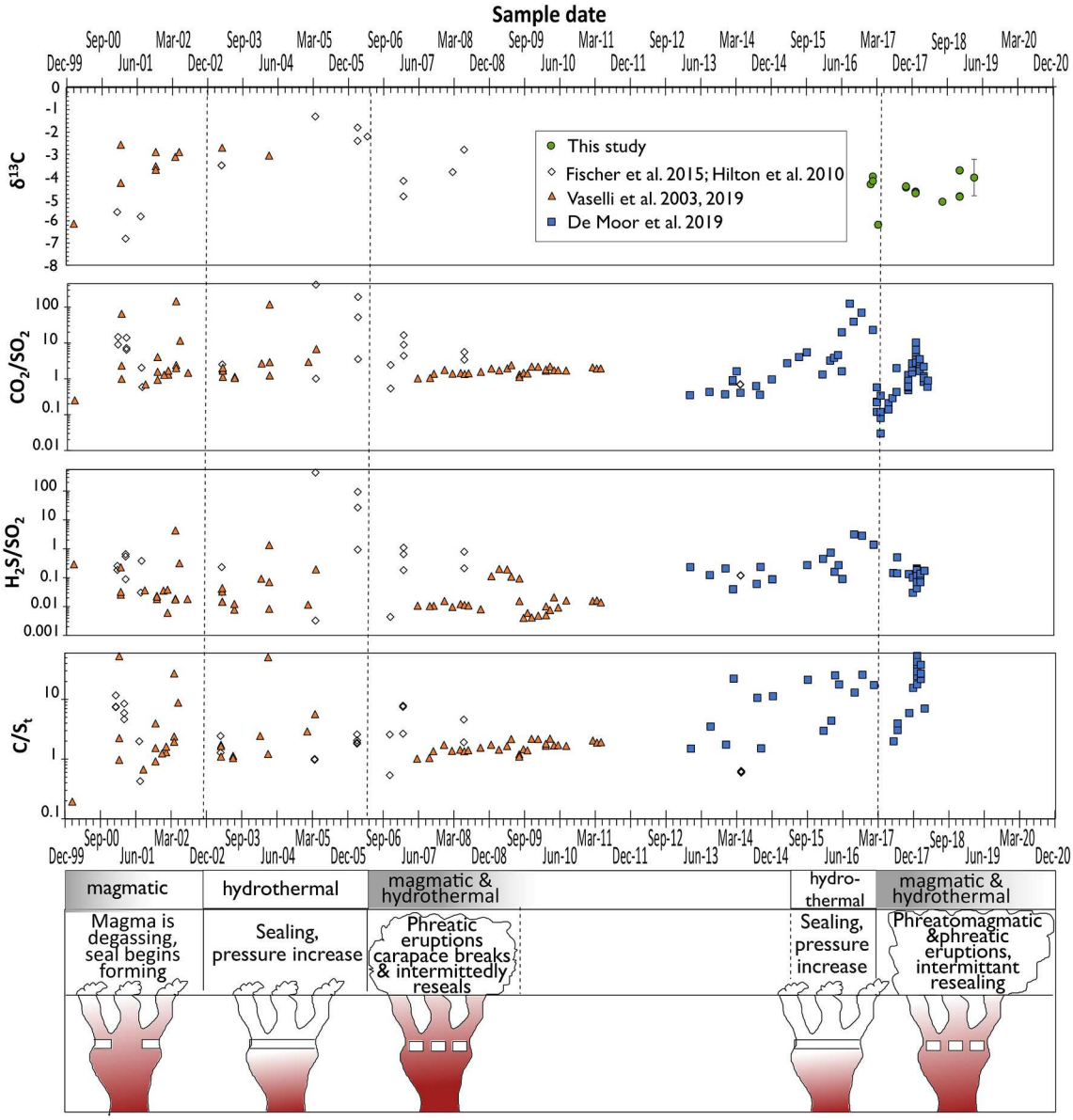

Fig. 6. Comparison of gas geochemistry from 1999 to 2019 at Poás volcano, Costa Rica, with a schematic model shown at the bottom. We have not applied our model to activity at Poás from 2009 to 2016 due to a lack of carbon isotopic data spanning this timeframe.

the volcanic CO_2. We found markedly similar $\delta^{13}C$ between the two techniques. Near-synchronous sampling across multiple sites at Poás has demonstrated little spatial variation in $\delta^{13}C$, allowing for multi-decadal comparison of carbon isotope systematics at Poás. We present results of $\delta^{13}C$ from fumarolic sampling spanning 2017 to 2019. A comparatively negative carbon isotopic value of −6.2 ‰ immediately prior to the April 2017 phreatomagmatic episode can be explained by our conceptual model, in which a broken hydrothermal seal allows volatiles from a degassed, pre-2006 magma to emit carbon with an isotopically light signature. Post-eruptive values return to pre-eruptive baseline values of −3.4 to −5.1 ‰. In 2018 to 2019, the values tend towards more positive $\delta^{13}C$ due to fluid-gas exchange governed by increasing temperature of the hydrothermal system as the seal reformed and periodic phreatic explosions provided fractures for fluid infiltration.

Declaration of Competing Interest

The authors declare that they have no known competing financial interests or personal relationships that could have appeared to influence the work reported in this paper.

Acknowledgments

The authors would like to thank the staff of the Parque Nacional Volcán Poás for coordinating our entry to the field site. FD is grateful for support from Vanier Canada. FD and JS were also supported by Discovery Grant funding from the Natural Sciences and Engineering Research Council of Canada, and by a seed grant from McGill University to purchase UAS. This work was also supported by funding from the Costa Rican Ley Transitorio 8933 and from Universidad Nacional, Costa Rica. Tobias Fischer and Geoffroy Avard are thanked for help in the field.

Appendix A. Supplementary data

Supplementary data to this article can be found online at https://doi.org/10.1016/j.jvolgeores.2022.107639.

References

Aiuppa, A., Bertagnini, A., Métrich, N., Moretti, R., Di Muro, A., Liuzzo, M., Tamburello, G., 2010. A model of degassing for Stromboli volcano. Earth Planet. Sci. Lett. 295, 195–204. https://doi.org/10.1016/j.epsl.2010.03.040.

Araujo, A., Kruijt, B., Nobre, A., Dolman, A., Waterloo, M., Moors, E., De Souza, J., 2008. Nocturnal Accumulation of CO_2 underneath a tropical forest canopy along a topographical gradient. Ecol. Appl. 18, 1406–1419.

Barry, P.H., de Moor, J.M., Giovannelli, D., Schrenk, M., Hummer, D.R., Lopez, T., Pratt, C.A., Segura, Y.A., Battaglia, A., Beaudry, P., Bini, G., Cascante, M., D'Errico, G., di Carlo, M., et al., 2019. Forearc carbon sink reduces long-term volatile recycling into the mantle. Nature 568, 487–492. https://doi.org/10.1038/s41586-019-1131-5.

Battaglia, A., de Moor, J.M., Aiuppa, A., Avard, G., Bakkar, H., Bitetto, M., Mora Fernández, M.M., Kelly, P., Giudice, G., Delle Donne, D., Villalobos, H., 2019. Insights into the mechanisms of phreatic eruptions from continuous high frequency volcanic gas monitoring: Rincón de la Vieja Volcano, Costa Rica. Front. Earth Sci. 6, 1–20. https://doi.org/10.3389/feart.2018.00247.

Boudoire, G., Rizzo, A.L., Di Muro, A., Grassa, F., Liuzzo, M., 2018. Extensive CO2 degassing in the upper mantle beneath oceanic basaltic volcanoes: first insights from Piton de la Fournaise volcano (La Réunion Island). Geochim. Cosmochim. Acta 235, 376–401. https://doi.org/10.1016/j.gca.2018.06.004.

Chiodini, G., Caliro, S., Aiuppa, A., Avino, R., Granieri, D., Moretti, R., Parello, F., 2011. First 13C/12C isotopic characterisation of volcanic plume CO_2. Bull. Volcanol. 73, 531–542. https://doi.org/10.1007/s00445-010-0423-2.

Chiodini, G., Pappalardo, L., Aiuppa, A., Caliro, S., Nazionale, I., Bologna, S., 2015. The geological CO_2 degassing history of a long-lived caldera. Geology 43, 767–770. https://doi.org/10.1130/G36905.1.

Christenson, B.W., Reyes, A.G., Young, R., Moebis, A., Sherburn, S., Cole-Baker, J., Britten, K., 2010. Cyclic processes and factors leading to phreatic eruption events: Insights from the 25 September 2007 eruption through Ruapehu Crater Lake, New Zealand. J. Volcanol. Geotherm. Res. 191, 15–32. https://doi.org/10.1016/j.jvolgeores.2010.01.008.

De Moor, J.M., Aiuppa, A., Pacheco, J., Avard, G., Kern, C., Liuzzo, M., Martínez, M., Giudice, G., Fischer, T.P., 2016. Short-period volcanic gas precursors to phreatic eruptions: Insights from Poás Volcano, Costa Rica. Earth Planet. Sci. Lett. 442, 218–227. https://doi.org/10.1016/j.epsl.2016.02.056.

De Moor, J.M., Stix, J., Avard, G., Muller, C., Corrales, E., Diaz, J.A., Alan, A., Brenes, J., Pacheco, J., Aiuppa, A., Fischer, T., 2019. Insights on hydrothermal - magmatic interactions and eruptive processes at Poás Volcano (Costa Rica) from high - frequency gas monitoring and drone measurements. Geophys. Res. Lett. 46, 1293–1302. https://doi.org/10.1029/2018GL080301.

Fischer, T.P., Lopez, T.M., 2016. First airborne samples of a volcanic plume for $\delta^{13}C$ of CO_2 determinations. Geophys. Res. Lett. 43, 3272–3279. https://doi.org/10.1002/2016GL068499.

Fischer, T.P., Ramírez, C., Mora-amador, R.A., Hilton, D.R., Barnes, J.D., Sharp, Z.D., Le Brun, M., De Moor, J.M., Barry, P.H., Füri, E., Shaw, A.M., 2015. Temporal variations in fumarole gas chemistry at Poás volcano, Costa Rica. J. Volcanol. Geotherm. Res. 294, 56–70. https://doi.org/10.1016/j.jvolgeores.2015.02.002.

Gerlach, T.M., Taylor, B.E., 1990. Carbon isotope constraints on degassing of carbon dioxide from Kilauea Volcano. Geochim. Cosmochim. Acta 54, 2051–2058. https://doi.org/10.1016/0016-7037(90)90270-U.

Giggenbach, W.F., 1975. A simple method for the collection and analysis of volcanic gas samples. Bull. Volcanol. 39, 132–145. https://doi.org/10.1007/BF02596953.

Giggenbach, W.F., 1984. Mass transfer in hydrothermal alteration systems-a conceptual approach. Geochim. Cosmochim. Acta 48, 2693–2711. https://doi.org/10.1016/0016-7037(84)90317-X.

Glamoclija, M., Garrel, L., Berthon, J., López-García, P., 2004. Biosignatures and bacterial diversity in hydrothermal deposits of Solfatara Crater, Italy. Geomicrobiol. J. 21, 529–541. https://doi.org/10.1080/01490450490888235.

Hanson, M.C., Oze, C., Werner, C., Horton, T.W., 2018. Soil $\delta^{13}C$-CO_2 and CO_2 flux in the H_2S-rich Rotorua hydrothermal system utilizing cavity ring down spectroscopy. J. Volcanol. Geotherm. Res. 358, 252–260. https://doi.org/10.1016/j.jvolgeores.2018.05.018.

Hilton, D.R., Ramírez, C.J., Mora-Amador, R., Fischer, T.P., Furi, E., Barry, P.H., Shaw, A. M., 2010. Monitoring of Temporal and Spatial Variations in Fumarole Helium and Carbon Dioxide Characteristics at Poás and Turrialba volcanoes, Costa Rica (2001–2009), 44, pp. 431–440.

Holloway, J., Blank, J., 1994. Application of experimental resultsto C-O-H species in natural melts. In: Carroll, M., Holloway, J. (Eds.), Volatiles in Magmas. Mineral Society of America, Washington, D.C., pp. 187–230

James, M., Carr, B., D'Arcy, F., Diefenbach, A., Dietterich, H., Fornaciai, A., Lev, E., Liu, E., Pieri, D., Rodgers, M., Smets, B., Terada, A., von Aulock, F., Walter, T., et al., 2020. Volcanological applications of unoccupied aircraft systems (UAS): Developments, strategies, and future challenges. Volcanica 3, 67–114. https://doi.org/10.30909/vol.03.01.67114.

Javoy, M., Pineau, F., Iiyama, I., 1978. Experimental determination of the isotopic fractionation between gaseous CO_2 and carbon dissolved in tholeiitic magma - a preliminary study. Contrib. Mineral. Petrol. 67, 35–39. https://doi.org/10.1007/BF00371631.

Keeling, C., 1958. The concentration and isotopic abundances of atmospheric carbon dioxide in rural areas. Geochim. Cosmochim. Acta 13, 322–334. https://doi.org/10.1016/0016-7037(58)90033-.

Liu, E.J., Aiuppa, A., Alan, A., Arellano, S., Bitetto, M., Bobrowski, N., Carn, S., Clarke, R., Corrales, E., de Moor, J.M., Diaz, J.A., Edmonds, M., Fischer, T.P., Freer, J., et al., 2020. Aerial strategies advance volcanic gas measurements at inaccessible, strongly degassing volcanoes. Sci. Adv. 6 https://doi.org/10.1126/sciadv.abb9103 eabb9103.

Lucic, G., Stix, J., Sherwood Lollar, B., Lacrampe-Couloume, G., Muñoz, A., Carcache, M. I., 2014. The degassing character of a young volcanic center: Cerro Negro, Nicaragua. Bull. Volcanol. 76, 1–23. https://doi.org/10.1007/s00445-014-0850-6.

Malowany, K., Stix, J., de Moor, J.M., Chu, K., Lacrampe-Couloume, G., Sherwood Lollar, B., 2017. Carbon isotope systematics of Turrialba volcano, Costa Rica, unsing a portable cavity ring-down spectrometer. Geochem. Geophys. Geosyst. 18, 2769–2784. https://doi.org/10.1002/2017GC006856.

Martelli, M., Caracausi, A., Paonita, A., Rizzo, A., 2008. Geochemical variations of air-free crater fumaroles at Mt. Etna: New inferences for forecasting shallow volcanic activity. Geophys. Res. Lett. 35, 2–7. https://doi.org/10.1029/2008GL035118.

Martínez, M., Fernández, E., Valdés, J., Barboza, V., Van Der Laat, R., Duarte, E., Malavassi, E., Sandoval, L., Barquero, J., Marino, T., 2000. Chemical evolution and volcanic activity of the active crater lake of Poas volcano, Costa Rica, 1993-1997. J. Volcanol. Geotherm. Res. 97, 127–141. https://doi.org/10.1016/S0377-0273(99)00165-1.

Mick, E., Stix, J., de Moor, J.M., Avard, G., 2021. Hydrothermal alteration and sealing at Turrialba volcano, Costa Rica, as a mechanism for phreatic eruption triggering. J. Volcanol. Geotherm. Res. 416, 107297 https://doi.org/10.1016/j.jvolgeores.2021.107297.

Paonita, A., Caracausi, A., Iacono-Marziano, G., Martelli, M., Rizzo, A., 2012. Geochemical evidence for mixing between fluids exsolved at different depths in the magmatic system of Mt Etna (Italy). Geochim. Cosmochim. Acta 84, 380–394. https://doi.org/10.1016/j.gca.2012.01.028.

Powers, J.S., 2006. Spatial variation of soil organic carbon concentrations and stable isotopic composition in 1-ha plots of forest and pasture in Costa Rica: Implications for the natural abundance technique. Biol. Fertil. Soils 42, 580–584. https://doi.org/10.1007/s00374-005-0054-5.

Ray, M.C., Hilton, D.R., Muñoz, J., Fischer, T.P., Shaw, A.M., 2009. The effects of volatile recycling, degassing and crustal contamination on the helium and carbon geochemistry of hydrothermal fluids from the Southern Volcanic Zone of Chile. Chem. Geol. 266, 38–49. https://doi.org/10.1016/j.chemgeo.2008.12.026.

Rizzo, A.L., Jost, H.J., Caracausi, A., Paonita, A., Liotta, M., Martelli, M., 2014. Real-time measurements of the concentration and isotope composition of atmospheric and volcanic CO_2 at Mount Etna (Italy). Geophys. Res. Lett. 41, 2382–2389. https://doi.org/10.1002/2014GL059722.Received.

Rizzo, A.L., Liuzzo, M., Ancellin, M.A., Jost, H.J., 2015. Real-time measurements of $\delta^{13}C$, CO_2 concentration, and CO_2/SO_2 in volcanic plume gases at Mount Etna, Italy, over 5 consecutive days. Chem. Geol. 411, 182–191. https://doi.org/10.1016/j.chemgeo.2015.07.007.

Rizzo, A.L., Pelorosso, B., Coltorti, M., Ntaflos, T., Bonadiman, C., Matusiak-Małek, M., Italiano, F., Bergonzoni, G., 2018. Geochemistry of noble gases and CO_2 in fluid inclusions from lithospheric mantle beneath wilcza góra (lower silesia, Southwest Poland). Front. Earth Sci. v. 6 https://doi.org/10.3389/feart.2018.00215.

Rodríguez, A., van Bergen, M.J., 2017. Superficial alteration mineralogy in active volcanic systems: an example of Poás volcano, Costa Rica. J. Volcanol. Geotherm. Res. 346, 54–80. https://doi.org/10.1016/j.jvolgeores.2017.04.006.

Rouwet, D., Mora-amador, R., Ramirez-umana, C.J., Gonzalez, G., Inguaggiato, S., 2017. Dynamic fluid recycling at Laguna Caliente Poa and during the 2006 – ongoing phreatic eruption cycle (2005–10). In: Ohba, T., Capaccioni, B., Caudron, C. (Eds.), Geochemistry and Geophysics of Active Volcanic Lakes, London, 437. Geological Society, Special publications, pp. 73–96.

Rowe, G.L., Brantley, S.L., Fernandez, M., Fernandez, J.F., Borgia, A., Barquero, J., 1992. Fluid-volcano interaction in an active stratovolcano: the crater lake system of Poás volcano, Costa Rica. J. Volcanol. Geotherm. Res. 49, 23–51. https://doi.org/10.1016/0377-0273(92)90003-V.

Rymer, H., van Wyk de Vries, B., Stix, J., Williams-Jones, G., 1998. Pit crater structure and processes governing persistent activity at Masaya Volcano, Nicaragua. Bull. Volcanol. 59, 345–355. https://doi.org/10.1007/s004450050196.

Rymer, H., Locke, C.A., Brenes, J., Williams-Jones, G., 2005. Magma plumbing processes for persistent activity at Poás volcano, Costa Rica. Geophys. Res. Lett. 32, 1–4. https://doi.org/10.1029/2004GL022284.

Rymer, H., Locke, C.A., Borgia, A., Martinez, M., Brenes, J., Van Der Laat, R., Williams-Jones, G., 2009. Long-term fluctuations in volcanic activity: Implications for future environmental impact. Terra Nova 21, 304–309. https://doi.org/10.1111/j.1365-3121.2009.00885.x.

Salvage, R.O., Avard, G., De Moor, J.M., Pacheco, J.F., 2018. Renewed explosive phreatomagmatic activity at Poás Volcano, Costa Rica in April 2017. Front. Earth Sci. 6, 1–18. https://doi.org/10.3389/feart.2018.00160.

Sandoval-Velasquez, A., Rizzo, A.L., Aiuppa, A., Remigi, S., Padrón, E., Pérez, N.M., Frezzotti, M.L., 2021. Recycled crustal carbon in the depleted mantle source of El Hierro volcano, Canary Islands. Lithos 400–401. https://doi.org/10.1016/j.lithos.2021.106414.

Sano, Y., Marty, B., 1995. Origin of carbon in fumarolic gas from island arcs. Chem. Geol. 119, 265–274.

Schipper, C.I., Moussallam, Y., Curtis, A., Peters, N., Barnie, T., Bani, P., Jost, H.J., Hamilton, D., Aiuppa, A., Tamburello, G., Giudice, G., 2017. Isotopically ($\delta^{13}C$ and $\delta z^{18}O$) heavy volcanic plumes from Central Andean volcanoes: a field study. Bull. Volcanol. 79 https://doi.org/10.1007/s00445-017-1146-4.

Shingubara, R., Tsunogai, U., Ito, M., Nakagawa, F., Yoshikawa, S., Utsugi, M., Yokoo, A., 2021. Development of a drone-borne volcanic plume sampler. J. Volcanol. Geotherm. Res. 412, 107197 https://doi.org/10.1016/j.jvolgeores.2021.107197.

Stix, J., de Moor, J.M., 2018. Understanding and forecasting phreatic eruptions driven by magmatic degassing: Earth. Planets and Space 70. https://doi.org/10.1186/s40623-018-0855-z.

Takahashi, H.A., Konohira, E., Hiyama, T., Minami, M., Nakamura, T., Yoshida, N., 2002. Diurnal variation of CO_2 concentration, $\Delta^{14}C$ and $\delta^{13}C$ in an urban forest: Estimate of the anthropogenic and biogenic CO_2 contributions. Tellus Ser. B Chem. Phys. Meteorol. 54, 97–109. https://doi.org/10.1034/j.1600-0889.2002.00231.x.

Tassi, F., Agusto, M., Vaselli, O., Chiodini, G., 2016. Copahue Volcano. In: Tassi, F., Vaselli, O., Caselli, A.T. (Eds.), Copahue Volcano. Springer-Verlag Berlin Heidelberg, Berlin-Heidelberg, pp. 119–139. https://doi.org/10.1007/978-3-662-48005-2.

Troll, V.R., Hilton, D.R., Jolis, E.M., Chadwick, J.P., Blythe, L.S., Deegan, F.M., Schwarzkopf, L.M., Zimmer, M., 2012. Crustal CO_2 liberation during the 2006 eruption and earthquake events at Merapi volcano, Indonesia. Geophys. Res. Lett. v. 39, 1–6. https://doi.org/10.1029/2012GL051307.

Tsunogai, U., Shingubara, R., Morishita, Y., Ito, M., Nakagawa, F., Yoshikawa, S., Utsugi, M., Yokoo, A., 2022. Sampling volcanic plume using a drone-borne SelPS for remotely determined stable isotopic compositions of fumarolic carbon dioxide. Front. Earth Sci. v. 10, 1–12. https://doi.org/10.3389/feart.2022.833733.

Vaselli, O., Tassi, F., Minissale, A., Montegrossi, G., Duarte, E., Fernández, E., Bergamaschi, F., 2003. Fumarole migration and fluid geochemistry at Poás Volcano (Costa Rica) from 1998 to 2001. In: Oppenheimer, C., Pyle, D., Barclay, J. (Eds.), Volcanic Degassing, 213. Geological Society, London, pp. 247–262. https://doi.org/10.1144/GSL.SP.2003.213.01.15.

Vaselli, O., Tassi, F., Fischer, T., Tardani, D., Fernandez, E., del Martinez, M., de Moor, J. M., Bini, G., 2019. The last eighteen years (1998–2014) of fumarolic degassing at the Poás Volcano (Costa Rica) and renewal activity. In: Tassi, F., Vaselli, O., Mora-Amador, R.A. (Eds.), Poás Volcano: The Pulsing Heart of Central America Volcanic Zone. Springer International Publishing, Switzerland, pp. 235–260. https://doi.org/10.1007/978-3-319-02156-0_10.

Venturi, S., Tassi, F., Bicocchi, G., Cabassi, J., Capecchiacci, F., Capasso, G., Vaselli, O., Ricci, A., Grassa, F., 2017. Fractionation processes affecting the stable carbon isotope signature of thermal waters from hydrothermal / volcanic systems : the examples of Campi Flegrei and Vulcano Island (southern Italy). J. Volcanol. Geotherm. Res. 345, 46–57. https://doi.org/10.1016/j.jvolgeores.2017.08.001.

Vogel, J.C., Grootes, P.M., Mook, W.G., 1970. Isotopic fractionation between gaseous and dissolved carbon dioxide. Z. Phys. 230, 225–238. https://doi.org/10.1007/BF01394688.

White, J.W.C., Vaughn, B.H., Michel, S.E., 2015. Institute of Arctic and Alpine Research (INSTAAR), Stable Isotopic Composition of Atmospheric Carbon Dioxide (13C and 18O) from the NOAA ESRL Carbon Cycle Cooperative Global Air Sampling Network, 1990-2014, Version: 2015-10-26. University of Colorado. ftp://aftp.cmdl.noaa.gov/data/trace_gases/co2c13/flask/.